Carbohydrate Polymers 115 (2015) 760–767

Contents lists available at ScienceDirect

Carbohydrate Polymers

journal homepage: www.elsevier.com/locate/carbpol

Nano-web structures constructed with a cellulose acetate/lithium chloride/polyethylene oxide hybrid: Modeling, fabrication and characterization

Atefeh Broumand[a,*], Zahra Emam-Djomeh[a,e,*], Faramarz Khodaiyan[a], Sasan Mirzakhanlouei[b], Driush Davoodi[c], Ali A. Moosavi-Movahedi[d]

[a] Transfer Phenomena Laboratory (TPL), Department of Food Science, Technology and Engineering, Faculty of Agricultural Engineering and Technology, University College of Agriculture and Natural Resources, University of Tehran, PO Box: 4111, 31587-11167 Karadj, Iran
[b] Department of Biotechnology, Research Center of Medical Plant—ACECR, Karadj, Iran
[c] Nanotechnology Laboratory, Department of Nanotechnology, Agricultural Biotechnology Research Institute of Iran, Karadj, Iran
[d] Institute of Biochemistry & Biophysics (IBB), University of Tehran, Tehran, Iran
[e] Center of Excellence for Application of Modern Technologies for Producing Functional Foods and Drinks

ARTICLE INFO

Article history:
Received 27 May 2014
Received in revised form 20 June 2014
Accepted 24 June 2014
Available online 1 July 2014

Keywords:
Nano-web structures
Cellulose acetate
Electrospinning
Molecular weight
Optimization

ABSTRACT

Electrospun nano-web structures (ENWSs) were successfully fabricated from ionized binary solution of cellulose$_{Mn30}$/polyethylene oxide$_{Mn200}$ (CA/PEO of 0.5–1.5). Final concentration of polymers was 12% (w/v) in the solution, and lithium chloride was used as ionizing agent. Response surface methodology (RSM) was applied to the optimize fabrication of ENWSs. Results of multiple linear regression analysis revealed that the solution properties and ENWSs morphology were strongly influenced by CA/PEO. An increase in PEO amount increased the viscosity which is a function of molecular weight, and as a result raised the entanglement of polymeric solution but decreased the surface tension that all support nanofibers fabrication. The size of nanofibers decreased with reducing PEO and LiCl concentration. Increasing the content of LiCl promoted the electrical conductivity (EC) value; however, junction zones were formed. The overall optimum region was found to be at combined level of 1.5% CA/PEO and 0.49% (w/v) LiCl.

1. Introduction

Over the past decade, some novel and important applications for using the electrospun nano-web structures (ENWSs) were found in various fields such as delivering vehicles for nutrients and nutraceuticals or other bioactive compounds, coating as fibrous film with highly porous nature and much greater surface area in comparison with conventional solution-cast films, protective nature for encapsulated active compound, carrier for antimicrobial compound, filtration media, biosensor application, and immobilization of enzyme on nanofibrous membrane (Kayaci & Uyar, 2012; Kriegel, Arrechi, Kit, McClements, & Weiss, 2008; Sozer & Kokini, 2009). ENWSs in comparison with other nano-scaled solid materials showed the enhanced interactions with their surrounding medium and thus can be considered as perfect substantial for exhibiting intrinsic features including open porous construction and continuous nano-web formation, which enable the easy accessibility of reactive compounds and prevent low mass diffusion in the different biosystems. Furthermore, ENWSs can be easily recovered and re-used for continuous operations (Kenawya, Abdel-Haya, El-Newehya, & Wnekb, 2009). Several methods have been developed to fabricate highly porous biodegradable scaffold including, solvent casting, emulsion freeze–drying, gas forming, particle leaching and three dimensional (3D) printing (Yao, Li, & Song, 2007), but the electrospinning technique has been recognized as an efficient and cost-effective method to fabricate nano-scale fibrous structures (Kriegel et al., 2008; Li, Lim, & Kakuda, 2009; Sozer and Kokini, 2009; Wongsasulak, Patapeejumruswong, Weiss, Supaphol, & Yoovidhya, 2010; Yao et al., 2007). In this process, a powerful electric field is used to form and depose non-woven nano-web from polymer solution, when a high electric field is applied on polymer solution leading to the droplet deformation (Yao et al., 2007; Wongsasulak et al., 2010). The composition of the solution (e.g.,

* Corresponding authors. Tel.: +98 261 224 8804.
E-mail addresses: atefe_borumand@ut.ac.ir (A. Broumand), emamj@ut.ac.ir (Z. Emam-Djomeh).

http://dx.doi.org/10.1016/j.carbpol.2014.06.055
0144-8617/

electrolytes, molecular weight and kind of polymers and solvents) in combination with the applied external electrical field could cause the ejection of a jet, if the electrostatic forces are able to overcome the surface-maintaining forces (Han, Son, Youk, & Park, 2008; Han, Youk, Min, Kang, & Park, 2008).

ENWSs fabricated by electrospinning show some surprising features such as very-large surface-area-to-volume ratio and flexibility in surface functionalities, compared to any other known form of the material (Kriegel et al., 2008). For some applications, the fibers may find uses as active packaging materials or as processing aids (e.g., catalytic reactors, membranes and filters) (Lala et al., 2007) and sensors (Ren et al., 2006; Sawicka, Gouma, & Simon, 2005).

Response surface methodology (RSM) is a collection of mathematical and empirical techniques useful for optimizing processes even in the presence of complex interactions (Sarlak, Farahm Nejad, Shakhesi, & Shabani, 2012). Central composite rotatable design (CCRD) is one of the successful factorial designs for the parameters optimization with a limited number of experiments and estimates the response surface (Huang et al., 2011). The objective of this study was to optimize the fabrication of ENWSs from cellulose acetate (CA) and polyethylene oxide (PEO) in binary solvent system of *N*,*N*-dimethylformamide (DMF)/dioxane (DOX). The combined effects of CA/PEO ratio and LiCl content on the viscosity, surface tension and electrical conductivity (EC) of prepared bicomponent solution, and morphology and diameter of the obtained ENWSs were investigated by RSM-CCRD. Based on the research done by Zhang and Hsieh (2008), a binary solvent system containing DMF/DOX is a suitable one for electrospinning of CA/PEO solution. Lithium chloride (LiCl) was used as an ionizing factor to investigate the solutions charge density on the morphology and diameter of fabricated ENWSs.

2. Materials and methods

2.1. Materials

CA (M_n = 30 kDa, 39.8 wt.% acetyl content) and PEO (M_n = 200 kDa) were purchased from Sigma Chemical Co. (St. Louis, MO, USA). DMF and DOX were provided by Panreac (Belgium) and Chem-lab NV (Spain), respectively. LiCl was obtained from Merck Chemical Co. (Darmstadt, Germany).

2.2. Solution preparation

According to CCRD, fixed proportion of each polymer and also a determined amount of LiCl (Table 1) in 1:1 DMF/DOX binary mixture were prepared by the dissolving. These mixtures were stirred for 4 h at 40 ± 1 °C under a constant stirring rate (300 ± 1 rpm) in order to obtain the homogenous and clear solutions. A 1:1 DMF/DOX mixture was a versatile solvent system to afford highly fiber generation from CA/PEO at a wide range of ratio. The ratio of the total polymers in the solvents was 12% (w/v). Then, the solutions were transferred to sealable brown bottles and stored at room temperature (23 ± 2 °C) up to be used for the electrospinning process and subsequent analyses.

2.3. Electrospinning process

A needle tip-to-collector distance of 23 cm and a voltage of 25 kV were applied. The flow rate of the solutions was controlled by a syringe pump (JMS, model SP 500, Japan). Electrospinning of each solution was done at 0.4 mL/h feed rate under ambient temperature. The mixed solutions were placed in a syringe (1 mL, gage 23, inner diameter 337 μm) that was coupled with a high voltage power supply. The grounded counter electrode was attached to an aluminum foil collector. Then, aluminum foil was separate from the collector and was used for the analysis of scanning electron microscopy (SEM).

2.4. Analytical methods for the prepared solutions

The viscosity measurements were performed at a constant shear rate of 36.69 s^{-1} at 40 ± 1 °C using a steady stress rheometer (Brookfield DV-II, LV Viscometer, USA). The viscosity of the solutions did not change for up to 70 h, indicating that the CA/POE solutions were very stable during the electrospinning process.

Surface tension of the solutions was measured at 40 ± 1 °C by the plate method using a Krüss K100 tensiometer (Krüss, Germany). Ten measurements were carried out for each solution in 120 s and the mean was used for data analysis.

The EC of solutions was triplicate measured at ambient temperature by using a digital conductometer (Metrohm model 660, Swiss).

2.5. Analytical methods for the developed nanofibers

The morphology of the fibrous membrane was observed using a SEM apparatus (KYKY-EM3200 SN:0056, China) as the mounted samples were sputtered with a thin layer of gold using a BAL-TEC SCD 005 sputter coater (BAL-TEC AG, Balzers, Liechtenstein). The average fiber diameters were determined by 50 measurements by Image J software (Windows version; National Institutes of Health, NIH).

2.6. Experimental design and statistical analysis

RSM-CCRD was applied to optimize the reaction conditions. This design was used to evaluate the effect of two most important independent variables including the CA/PEO ratio (X_1, 0.5–1.5, w/w) and LiCl (X_2, 0.25–0.75%, w/v) on the response variables of viscosity, surface tension, EC and fibers diameter. Based on the modified method of Zhang and Hsieh (2008) and a 2-factor-5-level CCRD (Table 1), 14 bicomponent polymer solutions were prepared. The center point was repeated six times to estimate the repeatability of the method (Gharibzahedi, Mousavi, Khodaiyan, & Hamedi, 2012). The response functions (y) were related to the coded variables (X_i, i = 1, 2) by a second-order polynomial using the following equation:

$$Y = \beta_0 + \beta_1 x_1 + \beta_2 x_2 + \beta_{12} x_1 x_2 + \beta_{11} x_1^2 + \beta_{22} x_1^2 \quad (1)$$

The coefficients of the polynomial equation were represented by β_0 (constant term), β_1 and β_2 (linear effects), β_{11} and β_{22} (quadratic effects) and β_{12} (interaction effects). The quality of the fit of polynomial model was expressed by the coefficient of determination R^2, adjusted R^2(R^2_{adj}), predicted R^2(R^2_{perd}) and adequate precision (ADP). ADP compares the range of the predicted values at the design points to the average prediction error. A ratio greater than 4 is desirable. The design was constructed with Design Expert statistical package (version 8.0.7.1 Stat-Ease Inc., Minneapolis, MN, USA). All experiments were carried out as the same time as possible to minimize the effect of experimental errors in the observed responses.

3. Results and discussion

3.1. Characterization of CA/PEO blend solutions

A set of preliminary studies were done to obtain the best condition for fabricating ENWSs (data not shown). The findings revealed that a polymer concentration of 12% (w/v) is the most appropriate amount in the solvent system containing 1:1 DMF/DOX. To determine the effect of mixture ratio and added LiCl on ENWS morphologies and diameters, some preliminary tests were performed.

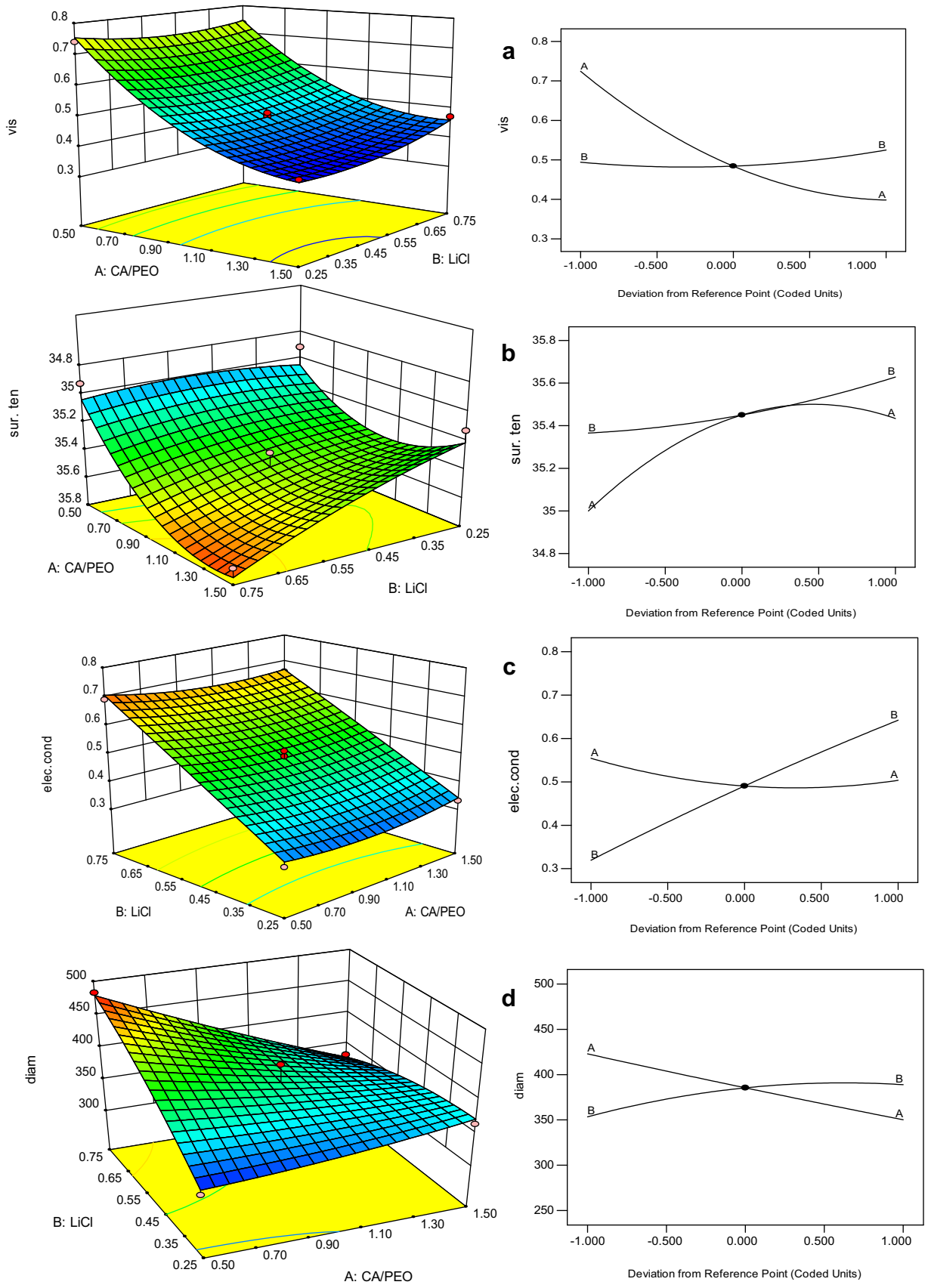

Fig. 1. 3D and perturbation plots showing the combined effect of CA/PEO and LiCl percentage on the viscosity (a), surface tension (b), EC (c), and diameter (d).

Table 1
Matrix of the central composite rotatable design (CCRD) and experimental data obtained for the response variables (mean ± SD).

Std	Independent variables		Response variables			
	CA/PEO (w/w)	LiCl (%, w/v)	Viscosity (Pa s)	Surface tension (mN/m)	EC (ms/cm)	Fibers diameter (nm)
1	0.50	0.25	0.740 ± 0.01	34.92 ± 0.24	0.360 ± 0.01	330.34 ± 41.85
2	1.50	0.25	0.397 ± 0.00	35.13 ± 0.18	0.331 ± 0.01	363.73 ± 69.03
3	0.50	0.75	0.735 ± 0.01	34.93 ± 0.21	0.691 ± 0.03	483.23 ± 51.45
4	1.50	0.75	0.470 ± 0.01	35.69 ± 0.15	0.660 ± 0.01	331.24 ± 61.55
5	1.00	0.50	0.489 ± 0.00	35.47 ± 0.21	0.492 ± 0.02	381.61 ± 32.41
6	1.00	0.50	0.480 ± 0.01	35.35 ± 0.23	0.469 ± 0.01	375.61 ± 37.47
7	1.00	0.50	0.491 ± 0.00	35.48 ± 0.20	0.473 ± 0.02	383.78 ± 30.72
8	0.29	0.50	0.886 ± 0.02	34.81 ± 0.25	0.561 ± 0.01	438.18 ± 27.62
9	1.71	0.50	0.394 ± 0.01	35.35 ± 0.14	0.539 ± 0.00	354.79 ± 37.80
10	1.00	0.15	0.517 ± 0.00	35.47 ± 0.22	0.249 ± 0.01	338.75 ± 40.64
11	1.00	0.85	0.556 ± 0.00	35.81 ± 0.21	0.748 ± 0.02	392.58 ± 26.57
12	1.00	0.50	0.485 ± 0.00	35.47 ± 0.21	0.486 ± 0.01	412.31 ± 35.91
13	1.00	0.50	0.497 ± 0.01	35.46 ± 0.23	0.492 ± 0.02	381.25 ± 30.23
14	1.00	0.50	0.463 ± 0.02	35.47 ± 0.21	0.511 ± 0.02	378.11 ± 32.11

Table 2
Table of ANOVA for the experimental variables as a linear, quadratic and interaction terms of each response variable and corresponding coefficients for the predictive models.

Source	DF	Viscosity (Pa s)		Surface tension (mN/m)		EC (ms/cm)		Fibers diameter (nm)	
		Sum of squares	*P*-value	Sum of squares	*P*-value	Sum of squares	*P*-value	Sum of squares	*P*-value
Model	5	0.2628	<0.0001	1.021	<0.0001	0.2574	<0.0001	21500.37	0.0001
Linear									
β1	1	0.2125	<0.0001	0.3757	<0.0001	0.0002	0.2589	6993.38	0.0002
β2	1	0.0019	0.0267	0.1380	0.0016	0.2519	<0.0001	4827.86	0.0007
Quadratic									
β11	1	0.0440	<0.0001	0.4013	<0.0001	0.0045	0.0004	151.87	0.3434
β22	1	0.0048	0.0030	0.0162	0.1298	0.0000	0.7791	873.35	0.0450
Interaction									
β12	1	0.0015	0.0408	0.0756	0.0076	0.0008	0.0343	8591.44	0.0001
Residual	7	0.0017		0.0385		0.0008		1029.47	
Lack-of-fit	3	0.0010	0.245^{ns}	0.0280	0.1264^{ns}	0.0001	0.8100^{ns}	278.91	0.7048^{ns}
Pure error	4	0.0006		0.0105		0.0006		750.56	
Total	13	0.2645		1.1145		0.2601		22683.81	
R^2		0.993		0.963		0.997		0.9543	
Adj-R^2		0.989		0.937		0.995		0.9217	
Pred-R^2		0.954		0.803		0.991		0.816	
CV		2.868		0.210		2.133		3.18	
ADP		43.53		20.05		66.47		17.71	

The effect of processing parameters such as voltage, flow rate and distance were investigated to obtain the best conditions. The results showed that a voltage of 25 kV, a flow rate 0.4 mL/h and a distance of 230 mm lead to a suitable target (data not shown). The effects of two independent variables of CA/PEO ratio (X_1) and LiCl content (X_2) and their interactions relationships on the response variables (Y) were studied. Analysis of variance (ANOVA) was performed to study the fitness of the constructed models and also to recognize the significant factors. The independent and dependent variables were suitably fitted by second-order polynomial equation. Table 2 gives the statistical significance, the linear and quadratic equations and the interaction effects calculated for each response. Fig. 1 depicts 3D and perturbation plots for the combined effect of CA/PEO and LiCl content on the viscosity (a), surface tension (b), EC (c), and diameter (d). These plots show how the response changes as each factor changes from the chosen reference point, with all other factors held constant at the reference value.

3.1.1. Viscosity

As considered in Table 2, the suggested model for viscosity (Y_1) was highly significant ($P < 0.0001$) with a non-significant lack of fitness ($P > 0.05$). Lack of fitness defines model divergence from the corresponding experimental values and the degree to which the predicted values are generated. Thus, a non-significant lack of fitness confirms the fitness of the model (Myers & Montgomery, 2002). The values of the R^2 (0.993), Adj-R^2 (0.989) and Pred-R^2 (0.954) also confirmed that the model was highly significant. The ADP value was 43.53 which shows a good signal-to-noise ratio for the studied models. Table 2 shows that the viscosity was highly affected by ratio of CA/PEO (X_1; $P < 0.0001$) and directly related to the linear effect of LiCl content (X_2; $P < 0.05$). Quadratic effects of CA/PEO ratio and LiCl concentration on the viscosity were significant ($P > 0.0001$ and $P > 0.01$, respectively). In addition, the mutual interaction of CA/PEO ratio with LiCl content was significant ($P < 0.05$). The viscosity of the ionized solution was significantly affected by polymers molecular weight (Wongsasulak et al., 2010). Clearly, an increase in PEO concentration of the solutions can raise the viscosity because of the higher molecular weight and as a result the fiber diameters increase (Table 1). In our previous work that was published in 2013, we investigated electrospinning of ionized CA/PEO solution in different molecular weight of 50 and 100, respectively. The ENWSs obtained from that bicomponent solution were finer but bead structure was observed in some cases (Broumand, Emam-Djomeh, Khodayan, Davoodi, & Mirzakhanlouei, 2014). Comparing the two types of nanofibers obtained from tow series polymer solutions (previous and current work) shows, increasing in molecular weight especially in PEO part of solution has a large effect on the size of electrospun nano-web (ENW) diameters. However, in the current study lower molecular weight of CA was used but presence of higher molecular weight of PEO had a remarkable effect on fiber diameters so the average size of the nanofibers form 100.68 in the previous study has increased to 381.82 in the current study. With the regard of viscosity's data in the previous and current study, it can be observed that the

viscosity values in the latter are higher, since viscosity is a parameter related to the molecular weight, this was expected to increase fiber diameters with increasing PEO part. Increasing in LiCl content significantly increased the solutions viscosity ($P<0.05$). This fact could be explained by strong electrostatic interactions between polymer chains in the solution (Kriegel et al., 2008). Fig. 1a shows an increase in viscosity with decreasing CA/PEO ratio whereas it leads to a reduction in the surface tension of the solution (Fig. 1b). The quadratic equation for the viscosity (Y_1) is given in the following equation:

$$Y_1 = 0.48 - 0.16X_1 + 0.015X_2 + 0.019X_1X_2 + 0.077X_1^2 + 0.025X_2^2 \quad (2)$$

3.1.2. Surface tension

Surface tension is a critical factor to fabricate uniform ENWSs. If the surface tension is very high, it may counteract the electrical forces hence the reduction in surface tension of the polymer solutions is a desirable condition for electrospinning (Greish, Meetania, Al Matroushib, & Al Shamsic, 2010; Wongsasulak et al., 2010). The predicted model for surface tension (Y_2) was highly significant ($P<0.0001$). As shown in Table 2, the surface tension was significantly affected by the linear and quadratic effects of CA/PEO ratio ($P<0.0001$), whit increasing CA/PEO ratio the surface tension significantly increased. Surface tension was linearly increased with increasing LiCl concentration ($P<0.01$), but its quadratic effect was not significant (Table 2). The surface tensions of solutions with higher LiCl concentration were not high like those with lower LiCl content although it had a significant effect. The R^2 value for the surface tension's equation was achieved to be 0.963. This indicates that only 3.7% of the total variation cannot be explained by the model. The values of Adj-R^2 and Pred-R^2 for this response were 0.937 and 0.803, respectively, which reveal adequacy of the constructed model. The fitted equation to predict surface tension behavior was given in the following equation:

$$Y_2 = 35.45 + 0.216X_1 + 0.131X_2 + 0.137X_1X_2 - 0.233X_1^2 \quad (3)$$

It can be observed that the variable with the largest effect on surface tension was linear terms of CA/PEO ratio and LiCl content followed by negative quadratic effect of CA/PEO ratio. Fig. 1b shows that reduction in CA/PEO ratio meaningfully reduces the surface tension value. Therefore, reduction behavior in surface tension level was found at a high PEO concentration (Cao & Kim, 1994). It could be due to the disruption of hydrogen bonds between cellulose chains by interfering PEO chains. Two molecules exhibit hydrogen bonding, but the extent of hydrogen bonding increases with the number of O—H bonds existing in each molecule (Petrucci, Harwood, Herring, & Madura, 2006). In lower surface tension values fabrication of the NWSs are supported and the diameter of them is reduced but the negative effect of higher PEO ratio on surface tension is not strong enough to overcome the increase in diameter caused by the higher molecular weight of PEO, also surface tension rises whit increasing the amount of LiCl. This fact may be attributed to higher charge density and electrical force of solution (Kriegel et al., 2008).

3.1.3. Electrical conductivity

The data presented in Table 2 indicate that the predicted model for EC was highly significant ($P<0.0001$). As can be observed, the EC of the solutions was significantly influenced ($P<0.0001$) by linear effect of LiCl content (Table 2). EC of the solutions rose with increasing LiCl concentration. Linear effect of CA/PEO ratio on the EC was not significant, but the quadratic effect of CA/PEO ratio was significant ($P<0.01$). The R^2, Adj-R^2 and Pred-R^2 values for EC found to be 0.997, 0.995 and 0.991. The ADP and CV amounts are also presented in Table 2. Following the calculation of the regression coefficient, the model for prediction of EC Y_3 was determined as

$$Y_3 = 0.49 + 0.178X_2 - 0.014X_1X_2 + 0.025X_1^2 \quad (4)$$

As expected the linear term of CA/PEO ratio X_1 had no significant effect on the EC of solution. In agreement with the results obtained by Wongsasulak et al. (2010), the results of present study showed that low EC is an effective factor to fabricate ENWSs and produce uniform and smooth fibers (Fig. 2a and h) and also could decrease the fiber diameters, but molecular weight is a more effective parameter on the fiber diameters. The addition of salt or electrolyte to the polymer solution increased the viscosity and surface tension of the solutions because columbic attraction draws ions and ionized molecule together and away from surface, so fiber diameters increased (Kriegel et al., 2008) in contrast. Kriegel et al. (2008) reported that higher EC can reduce the fiber diameter. They believed that in the higher EC more charge density is carried along the jet resulting in strong elongation forces, as a consequence, the jet is stretched more, reducing the fiber diameters.

3.2. Morphology of electrospun-nano web structures

SEM micrograph of ENW obtained from the current study showed a more uniform and bead-free structures compared with previous one (Broumand et al., 2014). This observation is attributed to the higher entanglement of polymeric solution due to higher viscosity as a function of higher molecular weight. Originally, the higher entanglement in polymeric solution supports the formation of nanofibers structure instead of bead structure; as a result, fiber textures appear more uniform and smooth. That is a key factor for the morphology of the ENWSs to use them in various sections because high surface-to-volume ratio is so important for the application of NWS and the formation of bead reduce this ratio. The presented model for fibers diameter (Y_4) was highly significant ($P<0.0001$). As shown in Table 2, there was a non-significant lack of fit that further validates the model ($P>0.05$). This fact can also be confirmed by the R^2 (0.954), Adj-R^2 (0.922) and Pred-R^2 (0.816) values. It was observed that the diameter of the ENWSs significantly depended on the PEO concentration ($P<0.0001$). The diameter was directly affected by linear effect of LiCl concentration ($P<0.01$). Even though the quadratic effect of CA/PEO ratio was not significant, but the quadratic effect of LiCl concentration was significant at $P<0.05$. The most significant effect on diameter value was revealed to be the interaction effect of CA/PEO and LiCl followed by the linear term of CA/PEO (Table 2). The fiber average size was significantly increased by decreasing CA concentration ($P<0.01$). ADP and CV values were also 17.70 and 3.18 for the fitted model, respectively. Multiple regression analysis was used to construct an empirical second order polynomial model and equation thus obtained by relating extent of conversion to coded levels of the variables was:

$$Y_4 = 385.36 - 29.57X_1 + 24.57X_2 - 46.34X_1X_2 - 10.88X_2^2 \quad (5)$$

It can be seen the largest effect on the fibers diameter was mutual interaction of independent variables. In general, fiber diameters increased with increasing viscosity, surface tension and EC. In which, the viscosity and EC were directly affected by molecular weight and solution charge density, respectively. In contrast, an increase in molecular weight reduces the surface tension. It has a positive effect on fiber diameters and reduces them. Results showed that the morphology and structure of the ENWSs were strongly affected by the ratio of CA/PEO and LiCl content. The finer ENWSs can be fabricated from ionized solutions using higher amount of CA and lower level of LiCl. The minimum, maximum

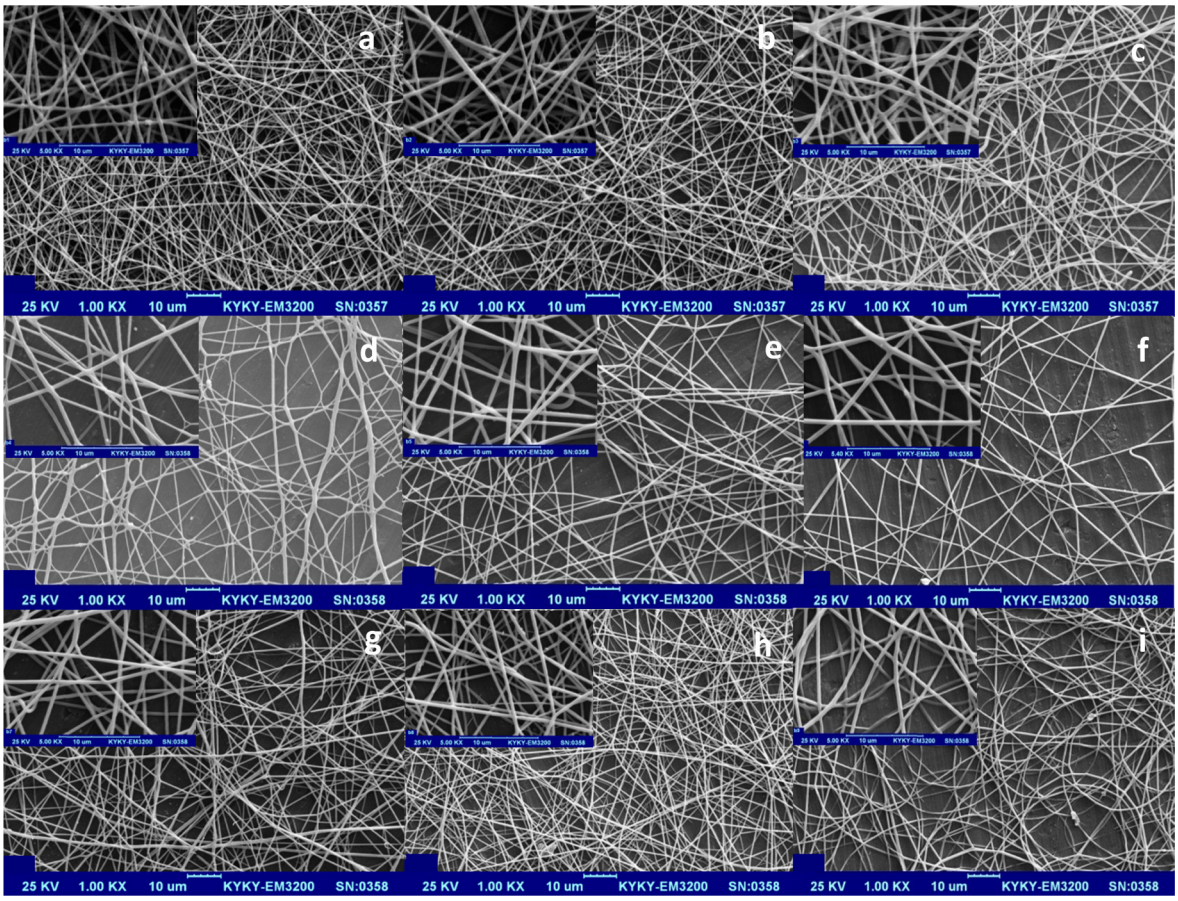

Fig. 2. SEM micrograph of electrospun solution containing various contents of CA/PEO ratio and LiCl%, (a) (run 1), (b) (run 2), (c) (run 3), (d) (run 4), (e) (central point runs), (f) (run 8), (g) (run 9), (h) (run 10), (i) (run 11).

and total average diameters for the fine homogeneous fibers were shown in Table 1. SEM images of the different ENWS samples at two magnifications have been presented in Fig. 2. For all samples, the ENWS images displayed well-defined structure without any junction zone except in Fig. 2c and d. The fiber diameters changes depending on the molecular weight and the polymer concentration (Kriegel et al., 2008). Fiber diameters increased with decreasing CA concentration or increasing molecular weight in the solutions. Higher concentration of PEO in solutions resulted in higher solution viscosity due to the higher polymer chain entanglement. The higher molecular weight led to produce larger fibers (Baek et al., 2011). Run 8 (CA/PEO: 0.29; LiCl 50%, w/v) was found to produce fibers with a mean average diameter of (438.18 ± 29.62). Increasing the LiCl concentration from 0.25 to 0.75% (w/v) led to an increase in the surface tension and EC of polymeric solutions, in which both increased the fibers diameter. In the case studied by Zhang and Hsieh (2008), fiber formation was influenced by chain length of polymers, their concentrations and mixing ratios and the used solvent. In current study, decreasing the ratio of CA/PEO significantly raised fiber diameters ($P < 0.01$) due to the greater chain length of PEO (200 kDa). The results showed that solution with high viscosity produced more uniform ENWSs. This result had a good agreement with finding obtained by Celebioglu and Uyar (2011). Higher molecular weight of polymer produced more uniform but larger fibers. Electrospinning of all solutions yielded highly uniform and bead-free ENWSs with average diameters of 331.24 ± 61.55 to 483.23 ± 51.45 nm. An interesting SEM image was obtained form run 4 (CA/PEO of 1.5 and LiCl 0.75%, w/v) (Fig. 2d). Junction zones can be seen in the ENWSs in Fig. 2d. It may be due to high EC of the initial solution (run 4). Formation of junction zones may reduce surface-to-volume ratio. This structure was observed in other runs including runs 3 (Fig. 2c), central points (Fig. 2e) and 8 (Fig. 2f) but less than the run 4 (Fig. 2d).

Increasing in the amount of LiCl could produce more junction zone (Fig. 2c). This result was in contrast with those obtained by Baek et al. (2011) who reported that decreasing the conductivity of solutions might increase the formation of junction zone in the ENWSs. But, Baek et al. (2011) suggested that formation of junction zone is a gift because the mechanical properties of ENWSs were significantly increased.

3.3. RSM optimization

The homogeneity of the ENWSs and their diameters were the main parameters that were used to optimize the process. As it can be seen in Fig. 2 the overall distribution of the most ENWSs are homogenous and thus expected to result in a homogenous pore size distribution. Overall optimization for the independent variables was carried out according to the information presented in Table 3. A CA/PEO ratio of 1.5 and a LiCl concentration of 0.49% (w/v) were determined as final optimum values for the independent variable (Table 3). The optimum values for the solution viscosity, surface tension, EC and fiber diameter were found to be 0.397 Pa s, 35.42 mN/m, 0.498 ms/cm, and 352.37 nm, respectively (Table 3). The 3D and perturbation plots for four studied responses as a function of CA/PEO ratio and LiCl content are shown in Fig. 3.

Table 3
Predicted optimum conditions and responses for the fabricated NFM.

Properties	Goal	Low	High	Optimum (predicted value)	Actual value
A:CA/PEO	In range	0.5	1.5	1.5	1.5
B:LiCl %	In range	0.25	0.75	0.49	0.49
Viscosity (Pa s)	Minimize	0.394	0.886	0.397	0.401 ± 0.018
Surface tension (mN/m)	Minimize	34.81	34.93	35.42	35.39 ± 0.23
EC (ms/cm)	Target	0.249	0.748	0.498	0.491 ± 0.016
Fibers diameter (nm)	Minimize	276.67	483.23	361.07	372.39 ± 31.27

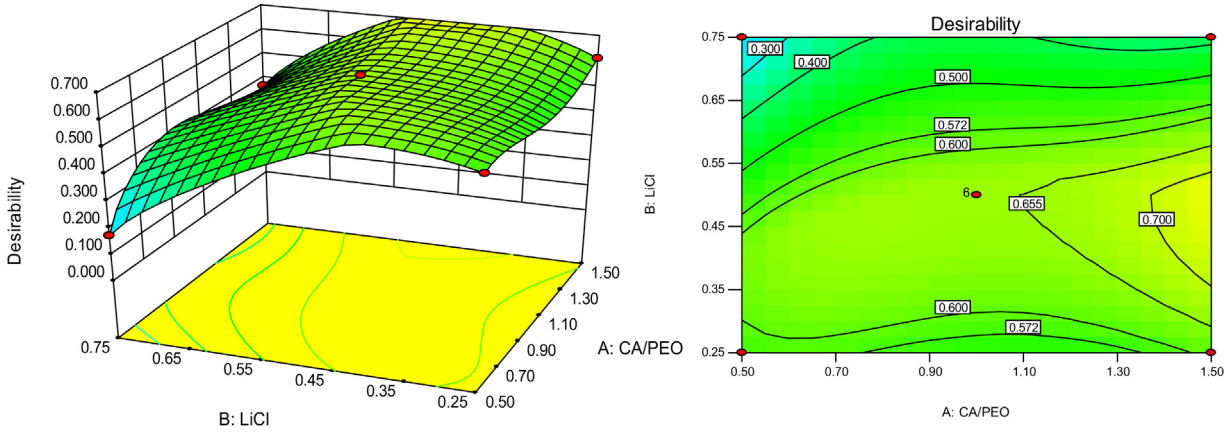

Fig. 3. The desirability 3D plot, obtained by overlaying 3D plots of four evaluated responses as a function of CA/PEO ratio and LiCl%.

3.4. Validation of predictive models

Validation is a perfect procedure to determine the model efficiency. The accuracy and potency of polynomial regression equations for the predicting optimum responses were examined using the suggested optimum conditions (CA/PEO of 1.5 and LiCl content of 0.49%, w/v) by repeating three additional experiments. The optimum results for output responses namely the viscosity, surface tension, EC and the diameter using Design-expert software were evaluated (Table 3). These results indicated that the viscosity, the surface tension, the EC and the diameter were obtained as 0.413 ± 0.017 Pa s, 35.31 ± 0.20 mN/m, 0.507 ± 0.012 ms/cm and 335.24 ± 30.61 nm, respectively. The confirmation experiments showed a good agreement between predicted and experimental data. Thus, response surface optimization suitably predicted the optimum conditions. This fact proposed that model equations had a high potential to determine the factors for fabricating suitable structure of ENW.

4. Conclusion

This research presented a successful modification and optimization of CA/PEO-ENWSs using LiCl as an ionizing agent. It was observed that the fiber structure and diameter were changed by varying the ratio of CA/PEO and the amount of LiCl. Morphological observation of ENW membranes with 0.75% (w/v) LiCl using SEM obviously revealed that junction zone formed in the structures and as a result surface-to-volume ratio decreased but may improve mechanical properties of ENWSs. This feature can broaden their application in different fields such as packaging and filtering. To improve the range of potential applications of nano-web, especial functionalization of them were investigated. Incorporation of functional components such as bioactive or drug with nanofibers can convert them into highly effective delivery systems; for example, fabrication of core–shell structures where active ingredients are incorporated in the core region of fiber. Sometimes they can be used for post-operative local chemotherapy. The release pattern of the active compounds can be easily manipulated through regulation and modulation of the formation conditions of their structure.

Acknowledgements

The authors are thankful to University of Tehran, center of excellence for the application of modern technologies for producing functional foods and drinks and Iranian Nano-technology Initiative Council.

References

Baek, W. I., Pant, H. R., Nama, K. T., Nirmala, R., Oh, H. J., Kim, I., et al. (2011). Effect of adhesive on the morphology and mechanical properties of electrospun fibrous mat of cellulose acetate. *Carbohydrate Research*, *346*, 1956–1961.

Broumand, A., Emam-Djomeh, Z., Khodayan, F., Davoodi, D., & Mirzakhanlouei, S. (2014). Optimal fabrication of nanofiber membranes from ionized-bicomponent cellulose/polyethylene oxide solutions. *International Journal of Biological Macromolecules*, *66*, 221–228.

Cao, B. H., & Kim, M. W. (1994). Molecular weight dependence of the surface tension of aqueous poly (ethylene oxide) solutions. *Faraday Discussions*, *98*, 245–252.

Celebioglu, A., & Uyar, T. (2011). Electrospun porous cellulose acetate fibers from volatile solvent mixture. *Materials Letters*, *65*, 2291–2294.

Gharibzahedi, S. M. T., Mousavi, S. M., Khodaiyan, F., & Hamedi, M. (2012). Optimization and characterization of walnut beverage emulsions in relation to their composition and structure. *International Journal of Biological Macromolecules*, *50*, 376–384.

Greish, Y. E., Meetania, M. A., Al Matroushib, E. A., & Al Shamsic, B. (2010). Effects of thermal and chemical treatments on the structural stability of cellulose acetate nanofibers. *Carbohydrate Polymers*, *82*, 569–577.

Han, S. O., Son, W. K., Youk, J. H., & Park, W. H. (2008). Electrospinning of ultra-fine cellulose fibers and fabrication of poly (butylene succinate) biocomposites reinforced by them. *Journal of Applied Polymer Science*, *107*, 1954–1959.

Han, S. O., Youk, J. H., Min, K. D., Kang, Y. O., & Park, W. H. (2008). Electrospinning of cellulose acetate nanofibers using a mixed solvent of acetic acid/water: Effects of solvent composition on the fiber diameter. *Materials Letters*, *62*, 759–762.

Huang, X. J., Chen, P. C., Huang, F., Ou, Y., Chen, M. R., & Xu, Z. K. (2011). Immobilization of *Candida rugosa* lipase on electrospun cellulose nanofiber membrane. *Journal of Molecular Catalysis B: Enzymatic*, *70*, 95–100.

Kayaci, F., & Uyar, T. (2012). Encapsulation of vanillin/cyclodextrin inclusion complex in electrospun polyvinyl alcohol (PVA) nanowebs: Prolonged shelf-life and high temperature stability of vanillin. *Food Chemistry*, *133*, 641–649.

Kenawya, E. R., Abdel-Haya, F. I., El-Newehya, M. H., & Wnekb, G. E. (2009). Processing of polymer nanofibers through electrospinning as drug delivery systems. *Materials Chemistry and Physics*, *113*, 296–302.

Kriegel, C., Arrechi, A., Kit, K., McClements, D. J., & Weiss, J. (2008). Functionalization, and application of electrospun biopolymer nanofibers. *Critical Reviews in Food Science and Nutrition*, *48*, 775–797.

Lala, N. L., Ramaseshan, R., Li, B. J., Sundarrajan, S., Barhate, R. S., Liu, Y. J., et al. (2007). Fabrication of nanofibers with antimicrobial functionality used as filters: Protection against bacterial contaminants. *Biotechnology and Bioengineering*, *97*, 1357–1362.

Li, Y., Lim, L. T., & Kakuda, Y. (2009). Electrospun zein fibers as carriers to stabilize (−) epigallocatechin gallate. *Journal of Food Science*, *74*, C233–C240.

Myers, R. H., & Montgomery, R. C. (2002). *Response surface methodology: Process and product optimization using designed experiments. Wiley series in probability and statistics* New York: Wiley.

Petrucci, R. H., Harwood, W. S., Herring, G., & Madura, J. (2006). *General chemistry: principles and modern application* (9th ed.). Prentice Hall.

Ren, G. L., Xu, X. H., Liu, Q., Cheng, J., Yuan, X. Y., Wu, L. L., et al. (2006). Electrospun poly(vinyl alcohol)/glucose oxidase biocomposite membranes for biosensor applications. *Reactive & Functional Polymers*, *66*, 1559–1564.

Sarlak, N., Farahmand Nejad, M. A., Shakhesi, S., & Shabani, K. (2012). Effects of electrospinning parameters on titanium dioxide nanofibers diameter and morphology: An investigation by Box–Wilson central composite design (CCD). *Chemical Engineering Journal*, *210*, 410–416.

Sawicka, K., Gouma, P., & Simon, S. (2005). Electrospun biocomposite nanofibers for urea biosensing. *Sensors and Actuators B: Chemical*, *108*, 585–588.

Sozer, N., & Kokini, J. L. (2009). Nanotechnology and its applications in the food sector. *Trends in Biotechnology*, *27*, 82–89.

Wongsasulak, S., Patapeejumruswong, M., Weiss, J., Supaphol, P., & Yoovidhya, T. (2010). Electrospinning of food-grade nanofibers from cellulose acetate and egg albumen blends. *Journal of Food Engineering*, *98*, 370–376.

Yao, Ch., Li, X., & Song, T. (2007). Electrospinning and crosslinking of zein nanofiber mats. *Journal of Applied Polymer Science*, *103*, 360–380.

Zhang, L., & Hsieh, Y. (2008). Ultra-fine cellulose acetate/poly (ethylene oxide) bicomponent fibers. *Carbohydrate Polymers*, *71*, 196–207.